npg

ORIGINAL ARTICLE

Role of gap junctions in the contractile response to agonists in the mesenteric artery of spontaneously hypertensive rats

Ke-Tao Ma[1,2,4], Xin-Zhi Li[2,3,4], Li Li[1,2], Xue-Wei Jiang[1], Xin-Yan Chen[1], Wei-Dong Liu[1], Lei Zhao[1,2], Zhong-Shuang Zhang[1,2] and Jun-Qiang Si[1,2]

To investigate the effects of hypertension on the changes in gap junctions between vascular smooth muscle cells (VSMCs) in the mesenteric artery (MA) of spontaneously hypertensive rats (SHRs). Whole-cell patch clamp, pressure myography, real-time quantitative reverse transcription PCR (qRT-PCR), western blot analysis and transmission electron microscopy were used to examine the differences in expression and function of the gap junction between MA VSMCs of SHR and control normotensive Wistar-Kyoto (WKY) rats. (1) Whole-cell patch clamp measurements showed that the membrane capacitance and conductance of *in-situ* MA VSMCs of SHR were significantly greater than those of WKY rats ($P<0.05$), suggesting enhanced gap junction coupling between MA VSMCs of SHR. (2) The administration of phenylephrine (PE) and KCl (an endothelium-independent vasoconstrictor) initiated more pronounced vasoconstriction in SHR versus WKY rats ($P<0.05$). Furthermore, 2-APB (a gap junction inhibitor) attenuated PE- and KCl-induced vasoconstriction, and the inhibitory effects of 2-APB were significantly greater in SHR ($P<0.05$). (3) The expression of connexin 45 (Cx45) mRNA and protein in the MA was greater in SHR versus WKY rats ($P<0.05$). The level of phosphorylated Cx43 was significantly higher in SHR versus WKY rats ($P<0.05$), although the expression of total Cx43 mRNA and protein in the MA was equivalent between SHR and WKY rats. Electron microscopy revealed that the gap junctions were significantly larger in SHR versus WKY rats. Increases in the expression of Cx45 and phosphorylation of Cx43 may contribute to the enhancement of communication across gap junctions between MA VSMCs of SHR, which may increase the contractile response to agonists.

INTRODUCTION

Gap junctions are the channel-forming structures between the membranes of two adjacent cells, which allow direct electrical communication between cells.[1,2] Gap junctions have a key role in the development, structure, physiology and pathology of many organs, particularly between vascular smooth muscle cells (VSMCs) in blood vessels.[3–7] For example, the coordination of vascular responses is essential for the control of normal vascular function. Cell-to-cell coupling via gap junctions is a vital component in this coordination. Gap junctions also allow the exchange of metabolites, ions and other messenger molecules between adjacent cells.[4,8,9] In vascular cells, gap junctions enable changes in membrane potential to be propagated electronically via coupling between VSMCs, endothelial cells (ECs) and a combination of both.[10] Significantly, electrical communication through gap junctions between VSMCs is essential for successful synchronization.[11]

Gap junctions are composed of proteins known as connexins (Cxs).[12,13] More than two dozen mammalian connexin genes have been identified,[14] of which several isoforms are expressed in the vascular system. The levels of connexin expression differ depending on the size and location of blood vessels as well as the species.[3] ECs predominantly express Cx37, Cx40 and some Cx43, whereas VSMCs express Cx43 and Cx45 as well as low levels of Cx37 and Cx40.[10,15] Changes in the expression levels of connexins are associated with the development of vascular diseases, such as hypertension, atherosclerosis and restenosis.[10] Changes in vascular connexin expression in spontaneously hypertensive rats (SHRs) and other hypertensive animal models have been reported.[3,10,16] However, the results of these studies are not consistent, which may be due to

[1]Department of Physiology, Medical College of Shihezi University, Shihezi, PR China; [2]The Key Laboratory of Xinjiang Endemic and Ethnic Diseases, Medical College of Shihezi University, Shihezi, PR China and [3]Department of Pathophysiology, Medical College of Shihezi University, Shihezi, PR China
[4]These authors contributed equally to this work.
Correspondence: Professor J-Q Si, Department of Physiology, Medical College of Shihezi University, Shihezi 832002, PR China.
E-mail: sijunqiang11@hotmail.com

differences in experimental models or the techniques used to study the mechanisms.[3,10,16] Furthermore, most of the studies on vascular connexin expression have focused on large elastic arteries[10,17] but not on resistant arteries or on gap junctions between VSMCs. In this study, whole-cell patch clamp, pressure myography, real-time quantitative reverse transcription PCR (qRT-PCR), western blot analysis and transmission electron microscopy were used to study the differences in function and expression of gap junctions between VSMCs of mesenteric arteries (MA) in SHRs and normotensive Wistar-Kyoto (WKY) rats.

MATERIALS AND METHODS

Animals
Twenty-week-old male SHR and WKY rats were used in this study. All protocols were approved by the Institutional Animal Care and Use Committee (IACUC) at the Medical College of Shihezi University and were consistent with the Guidelines for the Care and Use of Laboratory Animals published by the US National Institutes of Health (Public Health Service Policy on Humane Care and Use of Animals, DHEW Publication No. 96-01, PHS Policy revised in 2002). The rats were anesthetized and subsequently euthanized by exsanguination. Anesthesia was accomplished by intramuscular injection ($1 \, ml \, kg^{-1}$) of an anesthetic mixture of ketamine (500 mg), xylazine (20 mg) and acepromazine (10 mg) in 8.5 ml of H_2O. The third-order branch of the MA was harvested from the upper ileum mesentery, cleaned of adherent tissue and processed for whole-cell patch clamp recording, pressure myography, qRT-PCR, western blot analysis and transmission electron microscopic assessment. The blood pressure (BP) was measured non-invasively by tail-cuff plethysmography.

Tight-seal whole-cell patch clamp recording
The MA (approximately 0.4 mm long, 200 μm outer diameter) was transferred to a glass-bottom Petri dish filled with aerated external solution composed of the following (mM): NaCl 138, KCl 5, $CaCl_2$ 1.6, $MgCl_2$ 1.2, Na-HEPES 5, HEPES 6 and glucose 7.5. The preparation was secured at the bottom of the dish via the weight of a platinum strip on each end and digested with collagenase A ($1 \, mg \, ml^{-1}$) dissolved in the external solution at 37 °C for 15 min. After washing away the enzyme, the vessel was further cleaned to remove the adventitial tissue. The Petri dish was then placed onto the stage of an inverted microscope equipped with micromanipulators. The specimen was continuously superfused with the external solution ($0.2 \, ml \, min^{-1}$) at room temperature (22–25 °C).

Dissociated VSMCs were prepared from the MA of SHR and WKY rats. The cleaned arteries were incubated for 20 min in a low-Ca^{2+} buffer solution containing the following (mM): NaCl 142, KCl 5, $CaCl_2$ 0.05, $MgCl_2$ 1, Na-HEPES 4, HEPES 5 and glucose 7.5. The arteries were then cut into 1 mm segments and digested with a buffer solution containing papain ($1.5 \, mg \, ml^{-1}$), collagenase A ($2 \, mg \, ml^{-1}$), bovine serum albumin ($3.75 \, mg \, ml^{-1}$) and DL-dithiothreitol ($0.3 \, mg \, ml^{-1}$) at 37 °C for 20–25 min. After centrifuging ($67 \, g$ for 5 min) and replacing the supernatant with enzyme-free buffer three times, the preparation was triturated with a Pasteur pipette. The cell-rich suspension was transferred to a Petri dish with a poly-L-lysine-coated coverslip on the bottom. Once the dispersed cells had attached to the glass bottom, the dish was mounted on an inverted microscope and perfused with extracellular solution for whole-cell recording. VSMCs were identified by their characteristic spindle-shape.

Conventional whole-cell recordings were performed using an Axon 700B amplifier (Axon Instruments, Union City, CA, USA) as described previously.[18] Recording pipettes were pulled from borosilicate glass capillaries with filament using a Sutter Instruments P-97 puller. The pipette typically had a resistance of approximately 5 MΩ after being filled with internal solution containing the following (mM): κ-gluconate 130, NaCl 10, $CaCl_2$ 2, $MgCl_2$ 1.2, HEPES 10, ethylene glycol-bis [β-aminoethylether] N,N',N'-tetraacetic acid 5 and glucose 7.5. The membrane current or voltage signal was low-pass filtered at 10 kHz; the data were recorded on a PC equipped with a Digidata 1440A AD-interface and pClamp 10.2 software (Axon Instruments) at a sampling interval of 10, 20

or 100 μs. A Minidigi digitizer and Axoscope 10.2 software (Axon Instruments) were used to simultaneously perform gap-free recording at a sampling interval of 50 ms.

The seal resistance usually reached 1–20 GΩ before rupture of the membrane. Membrane rupture was achieved by a high-frequency buzz current and/or suction pressure from the pipette. The transient current over the membrane input capacitance (C_{input}) was routinely uncompensated to monitor and calculate the access resistance (R_a) and the membrane parameters on-line or off-line. The off-line calculation was performed with exponential fit to the capacitive current transients by employing commonly used equations. The C_{input} values for in-situ cells were calculated according to $C = Q/V$, in which the charge (Q) was obtained by a four-term exponential fit to the current transient elicited by a voltage step. The voltage clamping error introduced by the current (I) passing the R_a was corrected off-line according to the equation $V_m = V_C - IR_a$ (in which V_m is the actual clamping membrane voltage and V_c is the apparent command voltage), except where noted otherwise. Leak subtraction was performed off-line when appropriate.

Pressure myography
The MA was dissected out and placed in cold Krebs-Ringer bicarbonate solution containing the following (mM): NaCl 118, KCl 4.7, $MgSO_4$ 1.2, KH_2PO_4 1.2, $CaCl_2$ 2.5, $NaHCO_3$ 25 and glucose 11. The arteries were cannulated at both ends with glass micropipettes, secured using 12-0 nylon monofilament sutures, and placed in a microvascular chamber (Pressure Myograph System, DMT, Denmark). The chamber was superfused with Krebs-Ringer bicarbonate solution (pH 7.4, gassed with 95% O_2 and 5% CO_2) and maintained at 37 °C. The MA segment was pressurized to a constant transmural pressure of 60 mm Hg. The diameter was continuously determined using a video dimension analyzer and recorded using the DMT Vessel Acquisition Suite. Cumulative dose–response curves to PE (0.1–100 μM) and KCl (10–120 mM) were generated.

RNA extraction and real-time qRT-PCR
The MA was homogenized in 1 ml of TRIzol reagent, and the total RNA was extracted following the manufacturer's instructions (GE Healthcare-Amersham Biosciences, Pittsburgh, PA, USA). An aliquot (400 ng) of the resulting RNA was transcribed into complementary DNA using the Takara PrimeScript RT reagent (Takara Bio, Otsu, Japan). To measure the expression levels of selected genes, real-time qRT-PCR was performed using the ABI PRISM 7900HT Real-time qRT-PCR Detection System (ABI, Carlsbad, CA, USA). Each 10 μl reaction contained 5 μl of SYBR Green Master Mix (ABI), 1 μl of complementary DNA template (1–10 ng), 1 μl of a specific pair of primers (25 pM) and 3 μl of distilled water. Each reaction was performed in triplicate. The mRNA levels were normalized by the level of β-actin mRNA in each sample. The specific primers used were as follows: Cx43 forward, 5′-CCTGCTCATC CAGTGGTACA-3′; reverse, 5′-GGACGTGAGAGGAAGCAGTC-3′. Cx45 forward, 5′-GAAACGGAAGAGGACCATGA-3′; reverse, 5′-TTTTGGTTGGCT CTGCTCTT-3′.

Western blot analysis
The MA was homogenized in RIPA buffer (at a ratio of 100 mg of tissue to 200 μl of RIPA buffer) with freshly added protease inhibitor cocktail. The homogenates were incubated at 4 °C for 30 min and centrifuged at 12 000 g for 15 min at 4 °C. The supernatant was collected, and the protein concentration in the supernatant was determined. Protein aliquots (40 μg) were subjected to 4–15% Tris-glycine denaturing gradient gel electrophoresis. The proteins were then transferred to an nitrocellulose filter membrane. The membrane was hybridized with specific primary antibodies against connexin or phosphorylated connexin at 4 °C overnight. Subsequently, the membrane was incubated with an appropriated fluorescein-conjugated secondary antibody at room temperature for 1 h. Immunoreactive bands were detected using the ECL chemiluminescence reagent (GE Healthcare-Amersham Biosciences). The membrane was stripped following the manufacturer's instructions and labeled with β-actin antibody as an internal control. The intensities of the protein bands were analyzed using Quantity One software (Bio-Rad, Hercules, CA, USA).

Transmission electron microscopy

The MA was fixed in 2.5% glutaraldehyde in 0.1 mM sodium cacodylate buffer (pH 7.3) for 2 h. The specimens were then rinsed in buffer, fixed in cacodylate-buffered 2% OsO$_4$, stained en bloc with uranyl acetate, dehydrated with ethanol and embedded in epoxy resin following standard procedures. Thin sections were stained with uranyl acetate and lead citrate and examined with a Hitachi H600 electron microscope (Hitachi, Tokyo, Japan).

Source of reagents

All primary antibodies and the horseradish peroxidase-conjugated secondary antibody were obtained from Santa Cruz Biotechnology (Santa Cruz, CA, USA). The BCA protein assay kit was purchased from Pierce (St Louis, MO, USA). RIPA buffer, PE and 2-APB (a gap junction inhibitor) were purchased from Sigma (Rockford, IL, USA). 2-APB was dissolved in dimethyl sulfoxide as a stock solution before being further diluted with external solution to achieve the final concentrations. The final dimethyl sulfoxide concentration in solution was ⩽0.1%, which had no detectable effect on vasomotor activity.

Statistical analysis

The rats were age matched to minimize individual differences. The results are expressed as the mean ± SEM. Statistical analysis was performed using the SPSS (Statistical Package for the Social Sciences) 16.0 statistical software package (SPSS Inc., Chicago, IL, USA). The primary statistical tests were two-way and one-way analysis of variance. When the overall F test result of analysis of variance was significant, a multiple comparison Tukey test was applied. Student's t-test was used for comparisons between two means. The differences were considered significant when the P values were <0.05.

RESULTS

Basic parameters

The body weights of SHRs and WKY rats were 270 ± 6 g ($n = 55$) and 362 ± 10 g ($n = 60$), respectively ($P<0.01$). The blood pressure was significantly higher ($P<0.01$) in SHRs (198 ± 9 mm Hg) compared with WKY rats (112 ± 7 mm Hg).

Enhanced electrical coupling in MA VSMCs of SHR

Whole-cell recordings were performed on in-situ or dispersed MA VSMCs of SHRs and WKY rats. Step and ramp voltage commands from a holding potential of −40 mV were applied to measure the membrane properties of the cell. The current transients during the voltage steps showed a time course that fit poorly to a single-term exponential function in in-situ cells from SHRs and WKY rats (Figure 1); however, these current transients fit well to a four-term exponential function (not shown), indicating a multiple membrane source in the charging circuit or an electrical coupling of multiple cells in the vessel. In contrast, the dispersed VSMCs showed a step-induced fast capacitive current that fit well with a single-term exponential function (Figure 1).

The results of R_{input}, G_{input} and C_{input} of in-situ or dispersed VSMCs are summarized in Table 1. The G_{input} values of in-situ VSMCs were 16 and 8 times greater than those of the dispersed cells in SHR and WKY rats, respectively, suggesting a tighter electrical coupling in the recording circuit in SHR versus WKY rats. The C_{input} values of in-situ VSMCs were 17 and 11 times greater than those of the dispersed cells in SHR and WKY rats, respectively, further supporting the tighter coupling among VSMCs in SHR versus WKY rats.

Enhanced vasoconstriction by increased gap junction communication in SHRs

To examine the effects of hypertension on the smooth muscle-dependent vasomotor responses, phenylephrine (PE) and KCl were applied to the MAs of SHR and WKY rats. PE (0.1–100 μM) or KCl
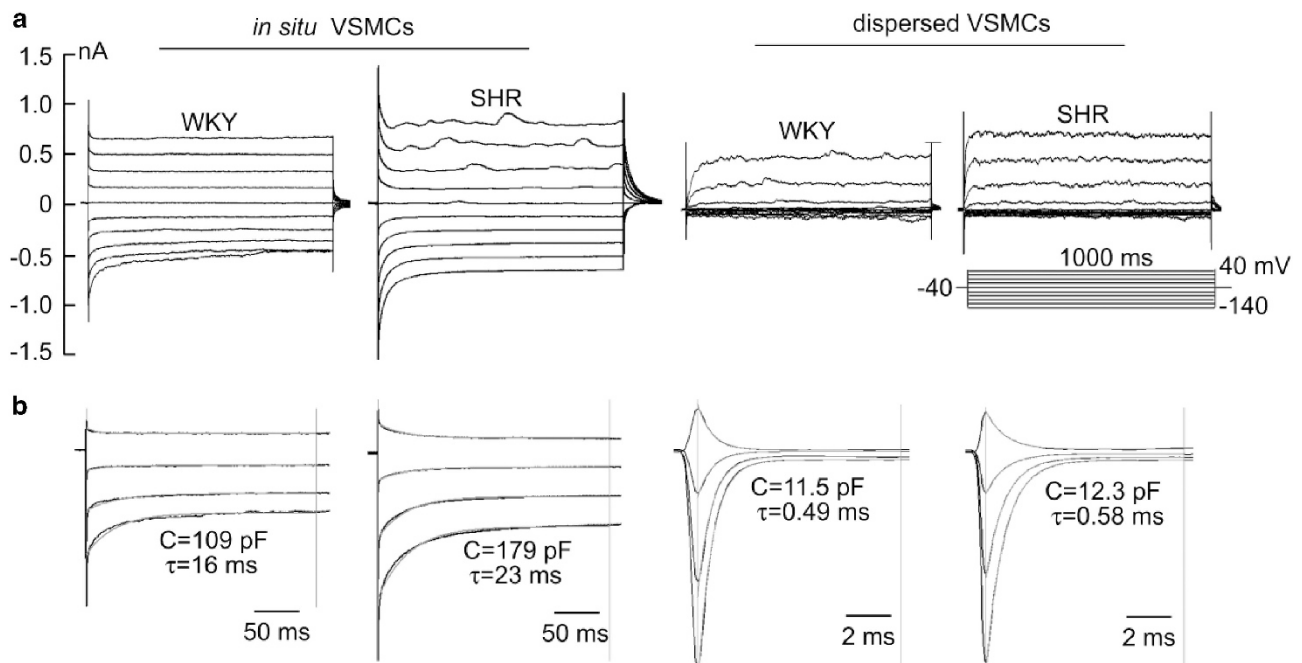

Figure 1 The electrical coupling of in-situ and dispersed mesenteric artery (MA) vascular smooth muscle cells (VSMCs) of spontaneously hypertensive rats (SHRs) and Wistar-Kyoto (WKY) rats. (**a**) Whole-cell current traces induced by voltage steps from the holding potential −40 mV in 20 mV increments on in-situ and dispersed VSMCs. (**b**) Time-scale-expanded presentation of the initial part of **a** (some traces omitted for clarity), showing that a single-term exponential function (red lines between two cursors) fitted poorly ($r<0.90$) with the current transients (black thin line) in in-situ VSMCs, but fit well ($r>0.98$) in dispersed VSMCs. 'C' and 'τ' membrane input capacitance and time constant for the bottom trace.

(10–120 mM) initiated concentration-dependent vasoconstriction of the MAs of SHR ($EC_{50} = 1.19\,\mu M$ for PE, 68 mM for KCl) and WKY rats ($EC_{50} = 1.09\,\mu M$ for PE, 67 mM for KCl). PE (1–100 μM) or KCl (60–120 mM) induced more pronounced vasoconstriction in SHRs versus WKY rats ($P < 0.05$; Figure 2).

Pre-incubation with the gap junction inhibitor 2-APB (100 μM for 5 min) inhibited PE- and KCl-induced vasoconstriction in both SHRs and WKY rats. The inhibitory effects of 2-APB on the vasoconstriction induced by PE (1–100 μM) or KCl (60–120 mM) were greater in SHR versus WKY rats ($P < 0.05$). Pre-incubation with 2-APB shifted the concentration–response curve of PE- or KCl-induced vasoconstriction downward. The estimated EC_{50} value was not significantly different between SHR ($EC_{50} = 2.40\,\mu M$ for PE, 50 mM for KCl) and WKY rats ($EC_{50} = 2.33\,\mu M$ for PE, 54 mM for KCl; Figure 2).

Increased vascular Cx43 and Cx45 expression in the MA of SHRs

The mRNA expression of Cx45 in the MA of SHR was significantly greater than that observed in WKY rats (Figure 3a). However, no

Table 1 Membrane properties of smooth muscle cells in whole-cell configuration *in-situ* and dispersed VSMCs of MA from SHR and WKY rats

Membrane property	In-situ VSMCs (n = 15)	Dispersed VSMCs (n = 14)
WKY rats		
R_{input} (MΩ)[a]	362 ± 85**	2443 ± 264
G_{input} (nS)[a]	4.01 ± 0.93*	0.48 ± 0.06
C_{input} (pF)[b]	114.0 ± 13.0*	10.0 ± 0.5
τ (ms)[b]	14.7 ± 0.7**	0.47 ± 0.07
SHR		
R_{input} (MΩ)[a]	142 ± 15**#	2400 ± 186
G_{input} (nS)[a]	7.7 ± 0.8**#	0.47 ± 0.05
C_{input} (pF)[b]	195.0 ± 47.0**#	11.2 ± 0.6
τ (ms)[b]	22.9 ± 0.7**#	0.51 ± 0.05

Abbreviations: MA, mesenteric artery; SHR, spontaneously hypertensive rat; VSMC, vascular smooth muscle cell; WKY, Wistar-Kyoto.
*$P < 0.05$, **$P < 0.01$ versus dispersed VSMCs.
#$P < 0.05$ versus WKY rats.
[a]Measured between −60 and −40 mV.
[b]Measured by a step from −40 to −100 mV.

significant difference was observed in the mRNA expression of Cx43 in the MAs of SHR and WKY rats (Figure 3b). Similar to the mRNA levels, the protein expression of Cx45 in the MA of SHR was significantly greater than that observed in WKY rats (Figure 4a). In contrast, the mRNA and protein expression of Cx43 in the MA did not differ between SHR and WKY rats (Figure 4b). However, the phosphorylation of Cx43 was significantly higher in the MA of SHRs compared with WKY rats (Figure 4c). Electron microscopy revealed that the size of the gap junctions in SHRs was significantly larger than that observed in WKY rats (Figure 5).

DISCUSSION

The goal of this study was to investigate the effect of hypertension on the communication of gap junctions among the VSMCs of the MA in SHRs. Our major findings were as follows: (1) the membrane capacitance and conductance of VSMCs of the MA in SHRs were significantly greater than those in WKY rats; (2) the PE- and KCl-induced vasoconstriction were significantly more pronounced in SHRs versus WKY rats, and the inhibitory effect of 2-APB on PE- and KCl-induced vasoconstriction was significantly greater in SHRs versus WKY rats; (3) the levels of Cx45 mRNA and protein and phosphorylated Cx43 in the MA were significantly greater in SHR versus WKY rats, and the size of the gap junctions between the MA VSMCs was larger in SHR versus WKY rats. These findings suggest that an increase in the expression of Cx45 and phosphorylation of
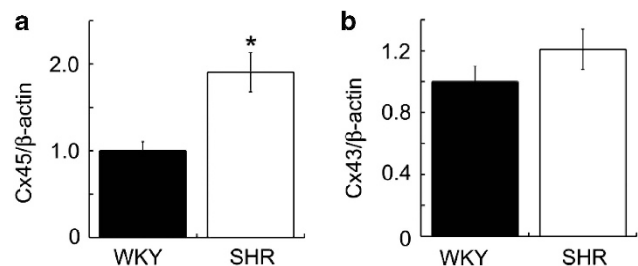
Figure 3 Levels of mRNA of connexin 43 (Cx43) and Cx45 in mesenteric artery of spontaneously hypertensive rats (SHRs) and Wistar-Kyoto (WKY) rats. (a, b) The level of mRNA of Cx45 and Cx43 respectively. *$P < 0.05$ versus WKY rats.
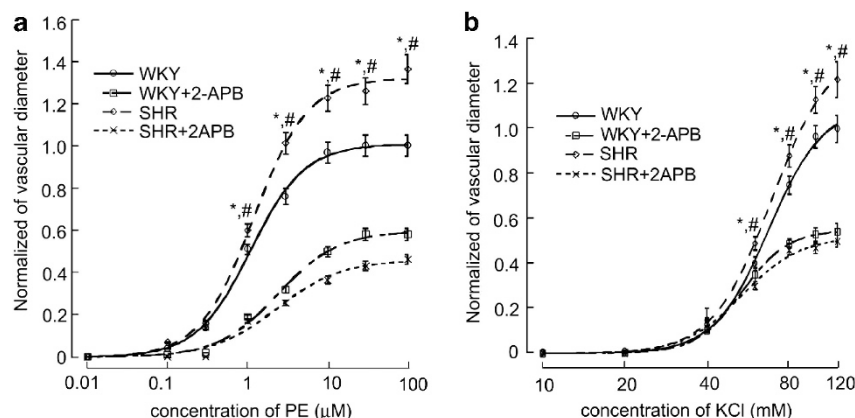
Figure 2 Dose–response curves of the effects of phenylephrine (PE) and KCl on vascular diameter of mesenteric artery (MA) of spontaneously hypertensive rats (SHRs) and Wistar-Kyoto (WKY) rats. (a) The effects of 2-aminoethoxydiphenyl borate (2-APB) on vasoconstriction induced by PE in SHRs and WKY rats, the vasoconstriction were both inhibited in SHRs and WKY rats, but more pronounced in SHRs. (b) The effects of 2-APB on vasoconstriction induced by KCl in SHRs and WKY rats, the vasoconstriction were both inhibited in SHRs and WKY rats, but more pronounced in SHRs. All data points are from 6 to 12 cells. *$P < 0.05$ versus WKY rats; #$P < 0.05$ the inhibited rate of 2-APB in SHR versus in WKY rats.

Cx43 may enhance the communication across gap junctions in the MA VSMCs of SHR to increase the contractile response to agonists. Compared with other studies, we used whole-cell patch clamping and pressure myography techniques to study the differences in gap junction function among VSMCs and to examine the role of gap junctions in the vasomotor tone of the MA in SHR. Our results confirm a relationship between VSMC gap junction function and the development of hypertension.[10]

The SHR strain was developed in the 1960s by Okamoto, who began breeding Wistar–Kyoto rats with high blood pressure. The two strains of rats have been separated since the 1960s. Therefore, in addition to blood pressure, other factors related to genetic background (for example, body weight and shape) may have been altered during the course of separation. Because the gap junctions between VSMCs have a major role in regulating vasomotor tone and vascular

resistance, we hypothesized that the increase in VSMC gap junction activity contributes to the development of hypertension in SHRs.

In this study, whole-cell recordings from VSMCs embedded in a segment of the MA were used to detect gap junction communication in SHRs and WKY rats. This novel technique was feasible for determining the function of gap junctions between VSMCs in a more physiologically relevant state (compared with dispersed VSMCs).[19] We also demonstrated that whole-cell recording from embedded VSMCs in arteriole segments is an accessible approach that can be used to electrophysiologically study various arteriolar preparations.[20,21] In Table 1, the G_{input}, C_{input} and τ of in-situ VSMCs were greater than those of dispersed VSMCs, suggesting a tighter electrical coupling among VSMCs in the recording circuit. Furthermore, the G_{input}, C_{input} and τ were greater in SHRs versus WKY rats, suggesting a tighter electrical coupling among VSMCs of the MA in SHRs versus WKY rats, confirming the results in Figure 1. The time course of the current transient during the voltage stepping poorly fit a single-term exponential function in the in-situ VSMCs; however, the dispersed VSMCs showed a step-induced current transient that fit well with a single-term exponential function, indicating multiple membrane sources in the circuit or an electrical coupling of multiple cells in situ. Hypertension can lead to hypertrophy of VSMCs,[22] and the C_{input} of a cell is positively correlated with the cell size. Although the C_{input} of in-situ VSMCs of SHRs was much higher than that of WKY rats, the C_{input} of a single VSMC from an SHR was the same as that of a single VSMC from a WKY rat, suggesting that the hypertrophy of VSMCs had little effect on gap junction communication.

Synchronization of vasomotor tone among VSMCs is critical for the function of blood vessels. The gap junction has a central role integrating VSMC function by coordinating changes in both membrane potential and intracellular Ca^{2+} between adjacent VSMCs.[23–25] Furthermore, gap junction communication among VSMCs is involved in myogenic vasomotor tone in resistance arteries.[26,27] Therefore, we examined whether the changes in the electrophysiological characteristics of VSMC gap junctions in SHR are consistent with the vascular response to endothelium-independent vasoconstrictors (PE and KCl). The maximal vasoconstrictive responses of the MA to PE and KCl were significantly greater in SHRs versus WKY rats. Consistent with our present findings, Anderson et al. reported that PE and KCl induced more pronounced vasoconstriction in the MA of rats with pregnancy-induced hypertension.[28,29] We further demonstrated that the gap junction inhibitor 2-APB elicited a greater inhibitory effect on PE- and KCl-
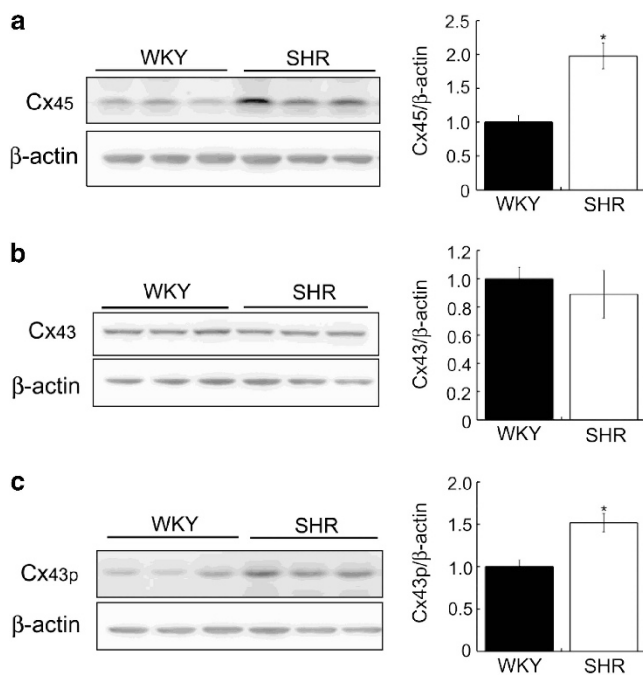
Figure 4 Levels of protein of connexin 43 (Cx43) and Cx45 in mesenteric artery of spontaneously hypertensive rats (SHRs) and Wistar-Kyoto (WKY) rats. (a–c) The level of protein of Cx45, Cx43 and Cx43p respectively. *$P<0.05$ versus WKY rats.
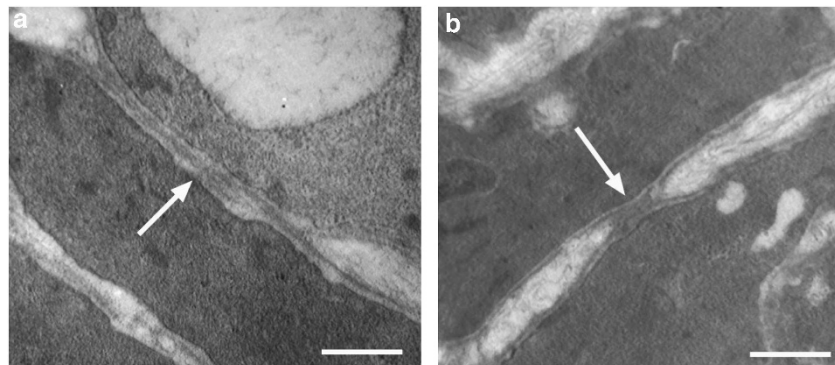
Figure 5 Eelectron micrographs of mesenteric artery sectioned longitudinally from spontaneously hypertensive rats (SHRs) and Wistar-Kyoto (WKY) rats. (a) SHR; (b) WKY rats. Individual gap junction profiles are identified by arrows. Bar = 0.5 μm.

induced vasoconstriction in SHRs versus WKY rats, suggesting that increased gap junction communication contributed to higher vasomotor tone in SHR.

Consistent with the changes in gap junction function, the levels of Cx45 mRNA and protein as well as phosphorylated Cx43 protein in the MA were significantly greater in SHRs versus WKY rats. Alonso et al. reported that Cx43 and Cx45 are expressed in the VSMCs of large and small arteries.[15,30] Cx45 was also increased in cerebral VSMCs in SHR.[17] Goto et al. and Tsai et al. found no changes in Cx43 in the MA VSMCs of SHR.[11,31] However, both increases and decreases in Cx43 have been reported in SHRs.[30,32] The discrepancy between these results may be associated with the particular animal species used, the distribution of the blood vessel and the vessel diameter.[3] In DOCA-salt, Goldblatt 2 kidney-1 clip (2K1C) and inhibition of NO synthase rat models of hypertension, intravascular pressure, increased angiotensin II and reduced NO are associated with the change in vascular connexin levels.[3] However, the levels of Cx43 and Cx45 protein were not significantly altered in cerebral vessels.[10,17] Furthermore, Li et al. reported that increased Cx45 in SHRs might not be due to elevated blood pressure or angiotensin II.[17] Therefore, the mechanisms of Cx43 and Cx45 changes in the MA of SHRs remain to be elucidated.

The vascular origin of many forms of hypertension depends on the modification of vasomotor tone. In VSMCs, the gap junction has an important role in synchronizing the changes in cytoplasmic Ca^{2+} in adjacent cells and in the overall development of vasomotor tone. Gap junctions between VSMCs may provide a preferred pathway for the conductance of vasomotor signals along the length of microvessels. Our current data demonstrate that increases in the expression of Cx45 and increases in phosphorylated Cx43 may enhance gap junction communication among VSMCs in resistant arteries of SHRs, which results in an increased vasoconstrictive response to agonists.

CONFLICT OF INTEREST

The authors declare no conflict of interest

1 McCracken CB, Roberts DC. Neuronal gap junctions: expression, function, and implications for behavior. Int Review Neurobiol 2006; 73: 125–151.
2 Sohl G, Maxeiner S, Willecke K. Expression and functions of neuronal gap junctions. Nat Rev 2005; 6: 191–200.
3 Figueroa XF, Isakson BE, Duling BR. Vascular gap junctions in hypertension. Hypertension 2006; 48: 804–811.
4 Figueroa XF, Isakson BE, Duling BR. Connexins: gaps in our knowledge of vascular function. Physiology (Bethesda, MD) 2004; 19: 277–284.
5 Griffith TM. Endothelium-dependent smooth muscle hyperpolarization: do gap junctions provide a unifying hypothesis? Br J Pharmacol 2004; 141: 881–903.
6 Sandow SL. Factors, fiction and endothelium-derived hyperpolarizing factor. Clin Exp Pharmacol Physiol 2004; 31: 563–570.
7 Jiang ZG, Nuttall AL, Zhao H, Dai CF, Guan BC, Si JQ, Yang YQ. Electrical coupling and release of K+ from endothelial cells co-mediate ACh-induced smooth muscle hyperpolarization in guinea-pig inner ear artery. J Physiol 2005; 564 (Pt 2), 475–487.
8 Segal SS. Regulation of blood flow in the microcirculation. Microcirculation 2005; 12: 33–45.
9 Juszczak GR, Swiergiel AH. Properties of gap junction blockers and their behavioural, cognitive and electrophysiological effects: animal and human studies. Prog Neuropsychopharmacol Biol Psychiatry 2009; 33: 181–198.
10 Brisset AC, Isakson BE, Kwak BR. Connexins in vascular physiology and pathology. Antioxid Redox Signal 2009; 11: 267–282.
11 Goto K, Rummery NM, Grayson TH, Hill CE. Attenuation of conducted vasodilatation in rat mesenteric arteries during hypertension: role of inwardly rectifying potassium channels. J Physiol 2004; 561 (Pt 1), 215–231.
12 Koval M. Pathways and control of connexin oligomerization. Trends Cell Biol 2006; 16: 159–166.
13 Laird DW. Life cycle of connexins in health and disease. Biochem J 2006; 394 (Pt 3), 527–543.
14 Sohl G, Willecke K. Gap junctions and the connexin protein family. Cardiovasc Res 2004; 62: 228–232.
15 Haefliger JA, Nicod P, Meda P. Contribution of connexins to the function of the vascular wall. Cardiovasc Res 2004; 62: 345–356.
16 Figueroa XF, Duling BR. Gap junctions in the control of vascular function. Antioxid Redox Signal 2009; 11: 251–266.
17 Li X, Simard JM. Increase in Cx45 gap junction channels in cerebral smooth muscle cells from SHR. Hypertension 2002; 40: 940–946.
18 Ma KT, Guan BC, Yang YQ, Nuttall AL, Jiang ZG. 2-Aminoethoxydiphenyl borate blocks electrical coupling and inhibits voltage-gated K+ channels in guinea pig arteriole cells. Am J Physiol 300: H335–H346.
19 Guan BC, Si JQ, Jiang ZG. Blockade of gap junction coupling by glycyrrhetinic acids in guinea pig cochlear artery: a whole-cell voltage- and current-clamp study. Br J Pharmacol 2007; 151: 1049–1060.
20 Quinn K, Beech DJ. A method for direct patch-clamp recording from smooth muscle cells embedded in functional brain microvessels. Pflugers Arch 1998; 435: 564–569.
21 Yamamoto Y, Fukuta H, Nakahira Y, Suzuki H. Blockade by 18beta-glycyrrhetinic acid of intercellular electrical coupling in guinea-pig arterioles. J Physiol 1998; 511 (Pt 2), 501–508.
22 Lacolley P, Regnault V, Nicoletti A, Li Z, Michel JB. The vascular smooth muscle cell in arterial pathology: a cell that can take on multiple roles. Cardiovasc Res 2012; 95: 194–204.
23 Christ GJ, Spray DC, el-Sabban M, Moore LK, Brink PR. Gap junctions in vascular tissues. Evaluating the role of intercellular communication in the modulation of vasomotor tone. Circ Res 1996; 79: 631–646.
24 Christ GJ, Moreno AP, Melman A, Spray DC. Gap junction-mediated intercellular diffusion of Ca2+ in cultured human corporal smooth muscle cells. Am J Phys 1992; 263 (2 Pt 1), C373–C383.
25 Christ GJ, Moreno AP, Parker ME, Gondre CM, Valcic M, Melman A, Spray DC. Intercellular communication through gap junctions: a potential role in pharmacomechanical coupling and syncytial tissue contraction in vascular smooth muscle isolated from the human corpus cavernosum. Life Sci 1991; 49: PL195–PL200.
26 Earley S, Resta TC, Walker BR. Disruption of smooth muscle gap junctions attenuates myogenic vasoconstriction of mesenteric resistance arteries. Am J Physiol 2004; 287: H2677–H2686.
27 Krüger O, Bény JL, Chabaud F, Traub O, Theis M, Brix K, Kirchhoff S, Willecke K. Altered dye diffusion and upregulation of connexin37 in mouse aortic endothelium deficient in connexin40. J Vascular Res 2002; 39: 160–172.
28 Anderson CM, Lopez F, Zhang HY, Pavlish K, Benoit JN. Reduced uteroplacental perfusion alters uterine arcuate artery function in the pregnant Sprague-Dawley rat. Biol Reprod 2005; 72: 762–766.
29 Anderson CM, Lopez F, Zhang HY, Shirasawa Y, Pavlish K, Benoit JN. Mesenteric vascular responsiveness in a rat model of pregnancy-induced hypertension. Exp Biol Med (Maywood, NJ) 2006; 231: 1398–1402.
30 Alonso F, Krattinger N, Mazzolai L, Simon A, Waeber G, Meda P, Haefliger JA. An angiotensin II- and NF-kappaB-dependent mechanism increases connexin 43 in murine arteries targeted by renin-dependent hypertension. Cardiovasc Res 87: 166–176.
31 Tsai ML, Watts SW, Loch-Caruso R, Webb RC. The role of gap junctional communication in contractile oscillations in arteries from normotensive and hypertensive rats. J Hypertens 1995; 13: 1123–1133.
32 Kansui Y, Fujii K, Nakamura K, Goto K, Oniki H, Abe I, Shibata Y, Iida M. Angiotensin II receptor blockade corrects altered expression of gap junctions in vascular endothelial cells from hypertensive rats. Am J Physiol 2004; 287: H216–H224.